Effect of Inhomogeneity on Spiral Wave Dynamics

Matthew Hendrey, Edward Ott,*,† and Thomas M. Antonsen, Jr.*

Department of Physics and Institute for Plasma Research, University of Maryland, College Park, Maryland 20742

(Received 17 April 1998)

The effect of weak inhomogeneity on spiral wave dynamics is studied within the framework of the two-dimensional complex Ginzburg-Landau equation description. The inhomogeneity gives spatial dependence to the frequency of spiral waves. This provides a mechanism for the formation of a dominant spiral domain that suppresses other spiral domains. The spiral vortices also slowly drift in the inhomogeneity, and results for the velocity are given. [S0031-9007(98)08283-0]

PACS numbers: 82.40.Ck, 47.32.Cc, 47.54.+r

Spiral waves occur in such diverse situations as cardiac arrythmias [1], reaction-diffusion systems (such as that describing the Belousov-Zhabotinsky reaction) [2,3], and slime mold colonies [4,5]. In this paper we consider the effect of an inhomogeneity of the supporting medium on spiral wave dynamics. For example, in the case of arrythmias, cardiac tissue is inherently inhomogeneous. For slime mold, an excitation inhomogeneity forms due to the sorting of the prestalk and prespore cells and the inhomogeneity results in spiral vortex motion [5]. As a potential example involving chemical reaction-diffusion systems, in Ref. [3] the chemical reaction rate was varied using its sensitivity to red laser light intensity. This could conveniently provide the means to create an inhomogeneity for a test of our theory by having the intensity vary over the entire system (other sources of reaction rate inhomogeneity are temperature inhomogeneity and inhomogeneity of the gel or porous glass medium in which chemical reaction-diffusion experiments are often done, etc.).

We find that, for a weak inhomogeneity, the evolution proceeds on distinct time scales. In particular, we find that, after spirals first form, the inhomogeneity causes certain spirals that are favorably located in the inhomogeneous medium to widen their domains, crowding out and sweeping away less favorably located spirals. In addition, the spiral vortices slowly drift with a velocity linearly related to appropriate gradients of the background medium properties.

Our studies of these effects are based on the two-dimensional complex Ginzburg-Landau equation,

$$\partial_t A = \mu A - (1 + i\alpha)|A|^2 A + (1 + i\beta)\nabla^2 A, \quad (1)$$

where $A(x, y, t)$ is complex. This equation provides a universal description for extended media in which the homogeneous state is oscillatory and near a Hopf bifurcation [6]. The equation is obtained as a balance between weak growth [$\mathrm{Re}(\mu)$], weak nonlinearity ($|A|^2 A$ term), and weak spatial coupling ($\nabla^2 A$ term). In the case of a homogeneous medium α and β are real constants, and μ can be set to unity by an appropriate rescaling of (1). A spiral wave solution to Eq. (1) then has the general form [7]

$$A(r, \theta, t) = F(r)\exp\{i[\sigma\theta - \omega_o t + \psi(r)]\}. \quad (2)$$

The topological charge $\sigma = \pm 1$ results in a $2\pi\sigma$ phase increment of A for a counterclockwise circuit around the vortex center ($r = 0$) where $A = 0$. For large r, the solution (2) is locally a plane wave of wave number k_o. Using the rescaling of μ to unity, the frequency ω_o satisfies the dispersion relation $\omega_o = \alpha + (\beta - \alpha)k_o^2$. The real functions $F(r) \equiv |A|$ and $\psi(r)$ have the following asymptotic behavior: $F \sim \psi' \sim r$ as $r \to 0$ and $F \to \sqrt{1 - k_o^2}$, $\psi' \to k_o$ as $r \to \infty$. It is found that, in an appreciable region of (α, β) parameter space, spiral wave solutions are stable, and that spiral waves naturally form from fairly arbitrary small initial perturbations from $A = 0$ [8]. In this regime, to which we restrict our considerations, A evolves toward a quasifrozen (i.e., very slowly evolving) state in which there are spiral wave domains with A approximately described by (2) separated by narrow walls, or "shocks" [9], with each domain having a vortex in its interior.

We now ask what is the effect on the above in the case of an inhomogeneity that occurs over a large length scale. In the expansion yielding (1) from a typical physical model such as a system of reaction-diffusion equations [6], the lowest order effect of the inhomogeneity is that the local frequency and growth rate of excitation depend on space. Thus we set

$$\mu = \gamma(x, y) + i\Omega(x, y), \quad (3)$$

where γ and Ω are slowly varying real functions of x and y (to lowest order α and β remain constant). Note that in a physical system the inhomogeneity will be significant if the spatial variation of the local non-normalized dimensional frequency or growth rate is comparable to the growth rate. Hence, nearer the Hopf bifurcation, a relatively small degree of inhomogeneity in physical parameters becomes significant. Consequently, we do not restrict the deviations of γ and Ω from their spatially averaged values to be small [10].

We begin by describing a numerical solution of (1) with inhomogeneity μ, Eq. (3). In the short time dynamics, just as in the homogeneous case ($\mu = 1$), a random initial condition consisting of many small amplitude plane waves rapidly leads to the formation of spiral wave domains distributed throughout the system. Figure 1 shows the time

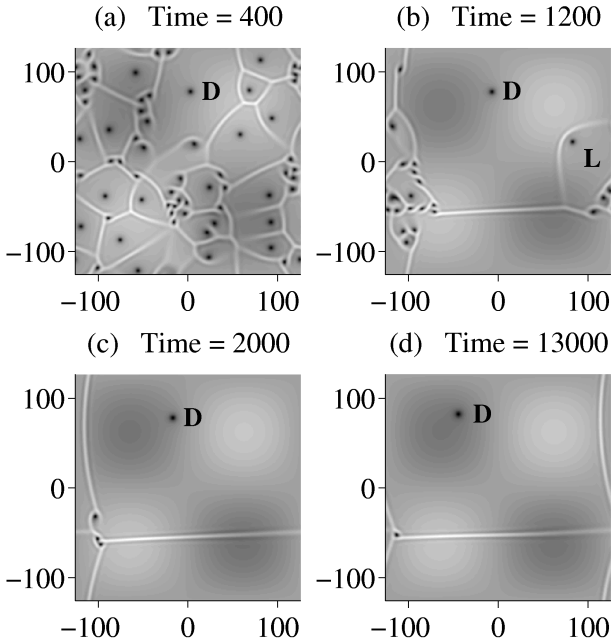

FIG. 1. Time evolution of $|A(x, y)|$.

evolution of the magnitude of A for the following parameters: $\alpha = 0.34$, $\beta = -1.45$, $\gamma = 1 + f(x, y)$, $f = c_1 \sin(x/40) \sin(y/40)$, $\Omega = c_2 \sin(y/40) \cos^2(x/80) + \omega_o f(x, y)$, $c_1 = 0.3$, $c_2 = 0.05$, and $\omega_o = 0.08\,145$. In Fig. 1 the darker regions have lower $|A|$. The domain walls are seen as ridges of lighter shade (larger $|A|$), and the vortices ($|A| = 0$) appear as the centers of dark spots. Figure 1(a) shows this system at time 400 to have many spiral vortices, just as in the homogeneous case. Whereas the homogeneous case results in spirals all with the same frequency ω_o, the inhomogeneity causes spirals at different locations to have different frequencies. Assuming slow spatial variations of μ allows a rescaling of (1) to give the asymptotic frequency for a spiral vortex at the location (x, y) to be

$$\omega(x, y) = \omega_o \gamma(x, y) - \Omega(x, y). \tag{4}$$

[For γ and Ω used in the simulation of Fig. 1 the range of the spiral vortex frequency from the (x, y) point of minimum ω to maximum ω is $\Delta\omega/\omega_o = 1.2$.] The frequency difference between waves emitted by vortices at different locations causes the domain walls between spirals to move. The domain walls must satisfy the condition that the phase of A matches across the domain wall [9,11]. Applying phase matching between two spirals, 1 and 2, assuming that both spiral vortices are far from the domain wall, gives a domain wall velocity of

$$v = \frac{\omega_1 - \omega_2}{k_{1,\perp} + k_{2,\perp}}, \tag{5}$$

where the reference positive direction of v points towards spiral 2 [11]. In (5), ω_1 and ω_2 are the spiral frequencies given by (4) evaluated at the locations of vortex 1 and vortex 2; $k_{1,\perp}$ and $k_{2,\perp}$ are the wave vector components normal to the domain wall for the solution to the local dispersion relation, $\omega_{1,2} = \alpha\gamma(\vec{x}) - \Omega(\vec{x}) + (\beta - \alpha)k_{1,2}^2$, evaluated at the domain wall. As a simplification, we note that in the situation to which we apply (5) below, $\vec{k}_1$ and $\vec{k}_2$ are approximately perpendicular to the domain wall at the intersection of the line joining vortices 1 and 2 with the moving domain wall. This simplification allows the phases for the two spirals to be written as $-\omega_{1,2}t + k_{1,2}r_{1,2}$, where $r_{1,2}$ is the distance from vortex 1(2) to the domain wall along the line between the two vortices. Equating the phases and differentiating with respect to time ($v = dr_1/dt = -dr_2/dt$) then gives (5) with $k_{1,2,\perp}$ replaced by $k_{1,2}$ for the domain wall velocity along the line joining the two vortices. (Note that this argument neglects motion of the vortices [such as the slow drift due to inhomogeneity, Eq. (7)].) Working in the parameter regime $\beta < \alpha$ gives $k_1, k_2 < 0$ (in order to have outgoing group velocity from a vortex), and we see from (5) that the domain of the spiral with the lowest frequency will grow (the wall velocity is away from the lower frequency vortex) while the domain with the larger frequency will shrink.

As time progresses, one spiral (or more depending on the precise details of the inhomogeneity) will dominate over the other spirals. In the parameter regime, $\beta < \alpha$, it will be the spiral with the lowest frequency that dominates. In our system, $\omega = \omega_o - c_2 \sin(y/40) \cos^2(x/80)$, and thus the dominant spiral (labeled D in Fig. 1) will be the spiral that forms closest to $(0, 20\pi)$. Indeed, looking at Figs. 1(a) and 1(b), we see that the dominant spiral is the spiral closest to $(0, 20\pi)$. Figure 1(b) also shows a lesser spiral (labeled L). We see that a domain wall has been pushed by D toward L, and in Fig. 1(b) this wall is now close to L. At this point, the lesser spiral L interacts strongly with the domain wall [12] and we observe that it is swept away at the speed of the domain wall,

$$v = \left| \frac{\omega_D - \omega_L}{k_D} \right|, \tag{6}$$

where the subscripts D and L stand for dominant and lesser spiral. [Equation (6) results from an argument similar to that used in deriving (5) except that now we take the L vortex to move with the same speed as the wall.] As time proceeds further, L is swept into a wall and occupies a negligible domain area. Furthermore, vortices of opposite charge embedded in the walls are observed to merge and annihilate [e.g., compare Figs. 1(b) and 1(c)]. Thus, after some time all the lesser spirals get swept away and the domain of the dominant spiral occupies nearly all the area. This is illustrated in Fig. 1(c).

The inhomogeneity not only creates a dominant spiral but also causes spiral vortices to drift [13]. This can be seen by comparing Fig. 1(b) to Fig. 1(d) and observing the dominant spiral's drift to the left. In the case of an inhomogeneity with a scale length much greater than one,

the drift will be linearly related to the gradient of the inhomogeneous $\mu = \gamma(x,y) + i\Omega(x,y)$. We recast the inhomogeneity μ into an inhomogeneity of the growth rate γ of homogeneous perturbations from $A = 0$ and the frequency ω of the spiral wave solution by defining $\omega(x,y)$ as in (4). The drift velocity of the spiral vortex depends only on local properties, i.e., $\nabla\gamma$ and $\nabla\omega$, of the inhomogeneity. The most general linear form of the drift velocity of a spiral vortex located at (x,y) can be expressed as

$$\vec{v}(x,y) = -\tilde{m}_{\omega,\parallel}\nabla\omega + \sigma\tilde{m}_{\omega,\perp}\hat{z}_o \times \nabla\omega - \tilde{m}_{\gamma,\parallel}\nabla\gamma + \sigma\tilde{m}_{\gamma,\perp}\hat{z}_o \times \nabla\gamma . \quad (7)$$

Rescaling the coefficients $\tilde{m}$ by introducing $m = \gamma\tilde{m}$, makes the m's independent of x and y and dependent on α and β only. We also find that $m_{\gamma,\perp} = 0$ and $m_{\gamma,\parallel} = (1 + \beta^2)$. To obtain this result consider for simplicity the velocity of a spiral vortex as it passes through $x = 0$ in the inhomogeneity $\Omega(x,y) = \epsilon_2 x$, $\gamma(x,y) = 1 + \epsilon_1 x$ which gives $\omega = \omega_o - (\epsilon_2 - \omega_o\epsilon_1)x$. In order to have a velocity only due to $\nabla\gamma$, set $\epsilon_2 = \omega_o\epsilon_1$ so that $\nabla\omega = 0$. We look for a solution with no drift along the perpendicular to $\nabla\gamma$ (y direction) and so transforming (1) to the comoving frame gives

$$\partial_t A - v_x\partial_x A = [1 + (\epsilon_1 + i\epsilon_2)(x + v_x t)]A - (1 + i\alpha)|A|^2 A + (1 + i\beta)\nabla^2 A . \quad (8)$$

Assuming that $v_x \sim \epsilon_1 \sim \epsilon_2$ is small, we neglect $O(\epsilon^2)$ terms and let $A(x,y,t) = e^{i(\kappa x' - \omega_o t)}\sqrt{\gamma}\,A'(x',y')$, where $x' = x + (\epsilon_1/4)(x^2 - y^2)$ and $y' = \sqrt{\gamma}\,y \cong (1 + \epsilon_1 x/2)y$. This then transforms (8) into

$$-i\omega_o A' - v_x\partial_{x'}A' = A' - (1 + i\alpha)|A'|^2 A' + (1 + i\beta) \times [\nabla'^2 A' + (2i\kappa + \epsilon_1)\partial_{x'}A'] .$$

Setting $\kappa = -\beta\epsilon_1/2$ and $v_x = -(1 + \beta^2)\epsilon_1$, cancels the $\partial_{x'}A'$ term and gives back Eq. (1). Thus (7) becomes [14]

$$\vec{v} = -(1 + \beta^2)\frac{\nabla\gamma}{\gamma} - m_{\omega,\parallel}\frac{\nabla\omega}{\gamma} + \sigma m_{\omega,\perp}\hat{z}_o \times \frac{\nabla\omega}{\gamma} . \quad (9)$$

The coefficients, $m_{\omega,\parallel}$ and $m_{\omega,\perp}$, are found numerically [15] using a procedure similar to that outlined in [16]. Figure 2 shows a typical plot of these coefficients as a function of α with $\beta = -1$ [15]. Using a similarity transformation [7] results in relations which transform from $m_{\omega,\parallel}(\alpha,\beta)$ to $m_{\omega,\parallel}(\alpha',\beta')$ and similarly for the perpendicular coefficient. These relations are

$$m_{\omega,\parallel}(\alpha',\beta') = \frac{(1 + \beta^2)\Sigma\Delta}{(1 + \omega_o\Delta)} + \Sigma m_{\omega,\parallel}(\alpha,\beta) , \quad (10)$$

$$m_{\omega,\perp}(\alpha',\beta') = \Sigma m_{\omega,\perp}(\alpha,\beta) , \quad (11)$$

where $\Delta = (\beta - \beta')/(1 + \beta\beta') = (\alpha - \alpha')/(1 + \alpha\alpha')$, $\Sigma = [(1 + \omega_o\Delta)/(1 + \beta\Delta)]^2$, and $\omega_o = \omega_o(\alpha,\beta)$. For example, Eqs. (10) and (11) convert knowledge of $m_{\omega,\parallel}$ and $m_{\omega,\perp}$ along the line $\beta = -1$ in parameter space (as in Fig. 2) to knowledge of $m_{\omega,\parallel}$ and $m_{\omega,\perp}$ at *any* point (α',β').

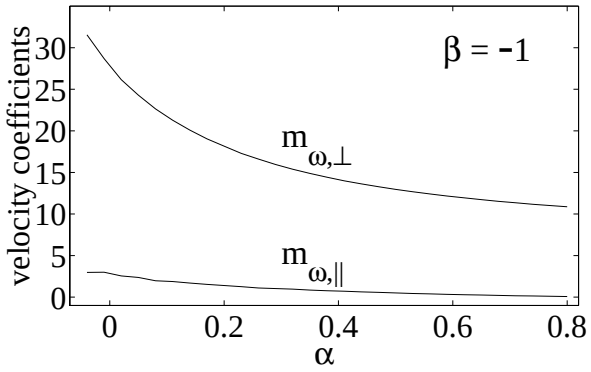

FIG. 2. Velocity coefficients $m_{\omega,\perp}$ and $m_{\omega,\parallel}$ plotted versus α with $\beta = -1$.

In Fig. 3(a), for the system used in Fig. 1, we plot the trajectory of the D spiral vortex from the simulation of (1) along with the trajectory of Eq. (9) starting with the spiral location from the simulation at time 650. At the end of the simulation the spiral has essentially reached a fixed point where $\vec{v}$ from (9) is zero [17]. Note that, at this fixed point, the frequency of the spiral is no longer the lowest available in the medium. If a new spiral could form at the initial location of the dominant spiral, it would overwhelm the present spiral. However, this does not happen since the

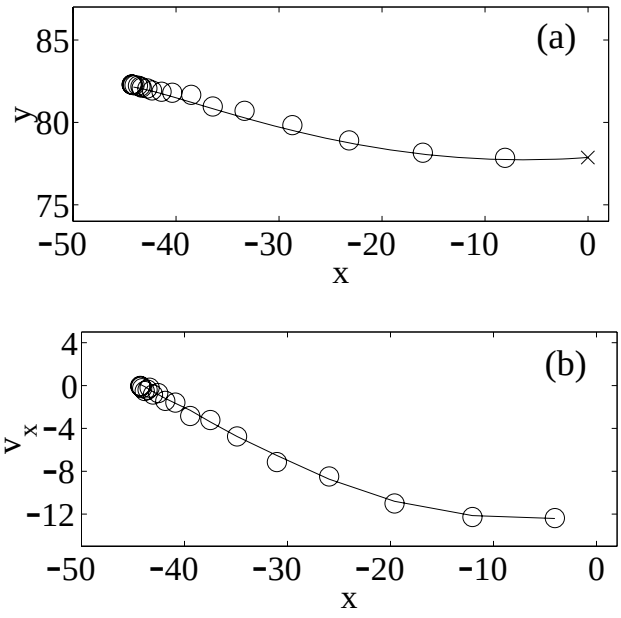

FIG. 3. (a) Vortex trajectory. × denotes the initial condition. The solid line is the result from the theory, Eq. (9), and the open circles are data from the numerical experiment. (b) Velocity in the x direction (in units of 10^{-3}) plotted as a function of x.

resulting configuration is stable, and there is no mechanism in (1) leading to the nucleation of new spirals. Figure 3(b) shows good agreement of the velocity in the x direction as a function of x between the theory from (9) (solid line) and the numerical simulation (open circles).

We note that our observation of two time phases of the motion, one where the primary role is played by wall motion [Eqs. (5) and (6)] and one where the primary role is played by vortex drift linear in the gradients [Eq. (9)], is due to the assumption of slow variation of γ and Ω. In particular, two vortices sufficiently far apart (e.g., L and D in Fig. 1) can have a substantial difference in frequency. The velocity v from (5) and (6) can then be substantial even for slow variation of γ and Ω. Thus the velocities from (5) and (6) can be much larger than that from (9), implying the observed evolution on two time scales. We also emphasize that the linear relation between the drift motion and local gradients [Eq. (9)] applies only for a slowly varying inhomogeneity and does not apply for more rapidly varying inhomogeneities [15,16(b),18].

In conclusion, an inhomogeneity of the medium in the complex Ginzburg-Landau equation has several effects. The frequency difference between spirals in the inhomogeneous system causes domain walls to move. For $\beta < \alpha$ ($\beta > \alpha$) this then leads to spiral domination of the lowest (highest) frequency spiral as the lesser spirals get swept away at the speed of the domain walls. The inhomogeneity results in slow spiral vortex drift with a drift velocity proportional to the gradient of the inhomogeneity.

M. H. thanks Michael Gabbay and Parvez Guzdar for the use of their computer simulation code. This work was supported by the Office of Naval Research.

*Also with Department of Electrical Engineering.
†Also with Institute for Systems Research.

[1] A. T. Winfree, Chaos **8**, 1 (1998), and references therein.
[2] (a) A. T. Winfree and W. Jahnke, J. Phys. Chem. **93**, 2823 (1989); (b) *Chemical Waves and Patterns,* edited by R. Kapral and K. Showalter (Kluwer Academic, Dordrecht, 1993); (c) for a review, see R. Kapral, Physica (Amsterdam) **86D**, 49 (1995).
[3] A. Belmonte and J.-M. Flesselles, Phys. Rev. Lett. **77**, 1174 (1996).
[4] A. J. Durston, Dev. Biol. **37**, 225 (1974).
[5] N. Nishiyama, Phys. Rev. E **57**, 4622 (1998).
[6] (a) M. C. Cross and P. Hohenberg, Rev. Mod. Phys. **65**, 851 (1993); (b) Y. Kuramoto, *Chemical Oscillations, Waves, and Turbulence* (Springer-Verlag, New York, 1984).
[7] P. Hagan, SIAM J. Appl. Math. **42**, 762 (1982).
[8] (a) H. Chate and P. Manneville, Physica (Amsterdam) **224A**, 348 (1996); (b) G. Huber, P. Alstrom, and T. Bohr, Phys. Rev. Lett. **69**, 2380 (1992); (c) I. S. Aranson, L. Aranson, L. Kramer, and A. Weber, Phys. Rev. A **46**, R2992 (1992).
[9] T. Bohr, G. Huber, and E. Ott, Physica (Amsterdam) **106D**, 95 (1997).
[10] In this Letter we have restricted consideration to the case $\gamma(x, y) > 0$ everywhere. The effect of $\gamma < 0$ in some regions will be dealt with in [15].
[11] K. Nam, E. Ott, M. Gabbay, and P. Guzdar, Physica (Amsterdam) **118D**, 69 (1998).
[12] M. Vinson, Physica (Amsterdam) **116D**, 313 (1998).
[13] A. M. Pertsov and Ye. A. Yermakova, Biophysics **33**, 364 (1988).
[14] The factor $(1 + \beta^2)$ in Eq. (9) also comes up in the related treatment of the motion of curved vortex filaments in the three-dimensional complex Ginzburg-Landau equation. M. Gabbay, E. Ott, and P. N. Guzdar, Phys. Rev. Lett. **78**, 2012 (1997); Physica (Amsterdam) **118D**, 371 (1998).
[15] Details of this calculation will be given in a longer report of this work [M. Hendrey, E. Ott, and T. M. Antonsen, Jr. (to be published)].
[16] (a) I. Aranson, L. Kramer, and A. Weber, Phys. Rev. Lett. **72**, 2316 (1994); (b) in *Spatio-Temporal Patterns in Nonequilibrium Complex Systems: NATO Advanced Research Workshop,* edited by P. E. Cladis and P. Palffy-Muhoray (Addison-Wesley, Reading, MA, 1995), p. 479. Section 7 of the latter paper provides results for the case of a strongly localized axisymmetric real inhomogeneity of extent of the order of a wavelength, $f_r(x, y) = 0.3 \exp[-(x^2 + y^2)/l^2]$, where $k_o l \cong 1$. They also discuss an inertialike effect of the spirals related to the core acceleration instability for large enough β. We defer discussion of this to Ref. [15].
[17] More generally, the equation for vortex motion, $d\vec{x}/dt = \vec{v}(\vec{x})$, with $\vec{v}$ given by (9) is an autonomous two-dimensional dynamical system and is expected to have fixed point attractors (as in our example) or limit cycle attractors (in which the vortex periodically circuits a closed path in space). [Another possibility, less often seen, is attraction to orbits homoclinic or heteroclinic to saddle fixed points. See, for example, M. W. Hirsch and S. Smale, *Differential Equations, Dynamical Systems, and Linear Algebra* (Academic Press, New York, 1974).] For $\vec{v} \in R^2$, by the Poincare-Bendixon theorem, these would be the typical attractors expected. The experimental results of Ref. [5] show both fixed point and limit cycle attractors. For $\vec{v} \in T^2$ (as in the case of periodic boundary conditions used for the computation in Fig. 1), quasiperiodic motion might also, in principle, be possible. With temporally periodic modulation of μ, Eq. (9) could also give chaotic vortex motion.
[18] I. V. Biktasheva, Y. E. Elkin, and V. N. Biktashev, Phys. Rev. E **57**, 2656 (1998); the authors relate the velocity of the spiral vortices to the perturbation through response functions. The response functions are shown numerically to be localized functions.